Ecological Economics 225 (2024) 108323

Contents lists available at ScienceDirect

Ecological Economics

journal homepage: www.elsevier.com/locate/ecolecon

Impact of *Fraxinus* snag fall on electric distribution and infrastructure stability: An empirical analysis

Erik Lyttek [a,*], Pankaj Lal [a], Brad Oberle [b], Ram S. Dubey [c], Eric Forgoston [a,d]

[a] Clean Energy and Sustainability Analytics Center, Montclair State University, 1 Normal Avenue, Montclair, NJ 07043, USA
[b] New York Botanical Garden, 2800 Southern Boulevard, Bronx, NY 10458, USA
[c] Department of Economics, Feliciano School of Business, Montclair State University, 1 Normal Avenue, Montclair, NJ 07043, USA
[d] Department of Applied Mathematics and Statistics, Montclair State University, 1 Normal Avenue, Montclair, NJ 07043, USA

ARTICLE INFO

Keywords:
Electric distribution
Fraxinus
Emerald Ash Borer (EAB)
Spatial modeling
Forest Inventory

ABSTRACT

With increasing climate variability and the movement of exotic pests and diseases, the rate of forest mortality has become an issue of global concern. Emerald Ash Borer (EAB), as one such pest, is causing the mass mortality of ash trees, *Fraxinus spp.*, thus leading to an ongoing surge in the number of snags across North America. Snags are dead-standing trees that pose an extant threat to nearby infrastructure and buildings. In this article, we evaluate the impacts which snags pose to electrical distribution infrastructure. New Jersey, a state with a high degree of urbanization, has an extensive electric grid located in forested areas. New Jersey is currently in the process of upgrading the electric distribution network, which will increase the height of electric distribution lines to increase resiliency and potential capacity. This article demonstrates a yearly risk assessment methodology for *Fraxinus* snags using an integrated GIS, differential equation, and applied regression model framework under two distribution network parameterizations. The framework is applied to three northern New Jersey counties (Warren, Sussex, and Morris), which are managed by one utility, New Jersey Central Power and Light, and which are home to most of New Jersey's *Fraxinus* trees.

1. Introduction

Emerald Ash Borer (EAB) is an Asiatic wood-boring pest that has been infesting North American ash trees (*Fraxinus spp.*) since the early 1990s. As a consequence of this infestation, much of the *Fraxinus* population has been destroyed, with the remaining trees at risk of dying. After the EAB infestation wave, a large number of standing dead *Fraxinus* are left in the canopy of affected regions as snags (Poland et al., 2015). These snags weaken the forest structure and pose a risk to both nearby trees and man-made infrastructure (Audley et al., 2021; Harmon and Bell, 2020).

Of particular interest is the infrastructure responsible for the distribution of electricity, as it frequently passes through forested areas home to mature *Fraxinus* (Hledik et al., 2017; Wilson et al., 2012). As the built and natural worlds must coexist, especially along the urban fringe forests of the environment, there exists a clear and present need to address these ecological-economic conflicts. The presence of EAB-induced dead *Fraxinus* increases the possibility of grid failure, and is therefore a pressing economic issue for both man-made and natural environments. Here we examine the region of Northwestern New Jersey where EAB has been actively eliminating *Fraxinus* stands for several years, leaving dead snags throughout the canopy (State of New Jersey Department of Agriculture).

Hardening the electric grid against snag fall may prove effective at preventing losses and unnecessary expenses while lowering the need to drastically interfere with the surrounding environment. There are two potential ways that this hardening may be achieved: (1) through regular trimming and cutbacks along electric distribution lines to prevent dead, or dying, trees from directly contacting the lines, or (2) by improving the infrastructure to reduce snag damage.

Currently, many New Jersey electric utilities are planning, or are in the process of planning, to upgrade their electric distribution network from the current 26 kV capacity distribution lines to 69 kV lines as part of their efforts to match the projections from the New Jersey Energy Master Plan and New Jersey Board of Public Utilities (NJBPU) et al. (2019). This distribution service upgrade is being done to both strengthen the resiliency of the state to wind events in the coastal areas, as well as increase the capacity of the grid to allow for increased adoption of electric-dependent technologies, like electric vehicles (EVs).

* Corresponding author.
E-mail addresses: ewlyttek@gmail.com (E. Lyttek), lalp@montclair.edu (P. Lal), boberle@nybg.org (B. Oberle), dubeyr@montclair.edu (R.S. Dubey), eric.forgoston@montclair.edu (E. Forgoston).

https://doi.org/10.1016/j.ecolecon.2024.108323
Received 14 September 2023; Received in revised form 8 June 2024; Accepted 24 July 2024
Available online 4 August 2024

As an added benefit, this upgrade in electrical capacity also increases the average height of distribution-level electric poles from 30 ft to 65 ft, with all power lines being placed at least 50 ft above ground level. This results in an increase of a minimum of 20 ft over the current height, which could significantly reduce the likelihood of a snag being within the critical range of the power line to cause an outage in general, allowing for less interaction between the forest and electrical infrastructure. An increase in the minimum height of the electric lines is a central facet of the scenario analysis performed in this study.

Previous studies on the impacts of other types of snags on infrastructure focus on small neighborhood to city level impacts, and rely on intensive sampling for the course of the study through on-the-ground measurements and methods (Bíl et al., 2017; Hughes et al., 2021; Poulos and Camp, 2010). This analysis seeks to provide further justification for both line maintenance schedules and the extension of electrical infrastructure upgrades at the regional level to address the large-scale disturbance caused by EAB (Public Service Electric & Gas Co. (PSE&G), 2007).

Rating infrastructure according to natural risk factors is not uncommon, but can be problematic due to intensive sampling methods that are often employed. This problem with infrastructure rating is especially true for electric distribution infrastructure that is often suspended in the tree canopy, and thus at elevated risk from nearby snags. It is therefore critical to maintain trees, shrubs, and other vegetation near and around electric distribution lines to prevent excess outages. By allowing trees and other vegetation to encroach upon essential infrastructure, the possibility of failure of the system during storms or even normal events is increased. The risk of tree falls can potentially cut power to residents for extended periods of time, which can have even greater economic impacts than damage to the system alone. In particular, outages can have severe effects on social and community health as well as the refrigerated food supply (Casey et al., 2020; Andresen et al., 2023; Liddiard et al., 2017). However, removing all trees along rights of way is improbable given the sheer length of distribution lines, the cost to landowners, and the character of the region (Hughes et al., 2021).

Numerous methods have been suggested to monitor tree-induced damage to electric infrastructure. One of the most common methods involves using intense tree surveys along small sections of infrastructure networks (Poulos and Camp, 2010). Others have used statistical and spatial data for a specified region (such as a city or county) under normal disturbance regimes over the course of years to decades to identify high-risk zones; data from these analyses may then be extrapolated for surrounding regions (Bíl et al., 2017). Monitoring methods also exist at the micro-scale to focus on strengthening the infrastructure itself and assess how often maintenance needs to be performed to prevent losses using the physical properties of the landscape and the state of the local infrastructure. This level of simulation can lead to positive outcomes on a small scale but is limited in scope due to the intense data collection requirements (Hughes et al., 2021).

According to Coder (2018) (Coder, 2014), the primary method by which trees fall is due to the wind blowing through the upper canopy, causing a rotational force on the trunk of the tree, pulling up on the root plate, which leads to tree-fall. However, wind damage is not correlated strongly with the fall rate of snags in the Eastern United States of America (USA), though it is correlated with other well-known snags in Northern Canada and the Western United States, where the mortality of one species results in much broader impacts to the canopy, such as large tracts of western pine species killed by mountain pine beetle (Oberle et al., 2018a; Audley et al., 2021; Harmon and Bell, 2020).

In relation to snags in the Eastern USA, Oberle et al. (2018a) constructed a multiple logistic regression analysis parameterized based on Forest Inventory and Analysis (FIA) snag data over the course of a decade. In their analysis, they found that air temperature, diameter at breast height (DBH), trees per hectare (TPH) species, and the region of the country were significant in determining when a snag would fall. Their method was able to predict which snag would fall 75% of the time over a five-year period. The largest influencing factors in their analysis for snag-fall were air temperature followed closely by the species' wood durability and the specimen's DBH.

With the impending loss of *Fraxinus* across the Northeastern USA, residents will need to brace for the budgetary impact this will have. This research addresses one aspect of these costs, specifically the vulnerability of electrical distribution infrastructure to the decay and fall of *Fraxinus*. Our methodology adapts the softmax and logistic regression model by Oberle et al. (2018a) to estimate the fall rate of snags across the study period. The regression model is coupled with an EAB spread model (Lyttek, 2023). Together, these models are used to (1) estimate the rate of snag fall in the study area and (2) estimate the rate at which utilities could see additional service interruptions and charges due to line clearing and repair.

2. Methods

For yearly snag falls and damages, the logistic regression model developed by Oberle et al. (2018a) has been adapted and coupled with an EAB spread model initially developed in Lyttek et al. (2019), and further developed and expanded in Lyttek (2023). Together, these methods/models are used to (1) estimate the rate of snag fall in the study area, and (2) estimate the rate at which utilities could be affected by service interruptions. The interruptions increase economic costs due to line clearing and repair in northern New Jersey, where the landscape is heavily forested and populated.

To estimate the rate of snag introduction, the mortality of *Fraxinus* caused by EAB is tracked using an EAB spread model (Lyttek, 2023). The model allows one to determine the amount, in square meters of basal area per hectare, and location of damaged trees as a yearly output. These mortally damaged *Fraxinus* trees become the source of new snags, which are assumed to belong to the first decay class (see Table 1 for decay class descriptions) as defined by the FIA (Forest Inventory and Analysis, 2022).

Over time, these new snags will fall, and this could cause damage to existing infrastructure. However, predicting when snags will fall is not a trivial matter. The adapted regression model from Oberle et al. (2018a) is parameterized using additional data that has become available since the time the original model was developed.

First, a sample of snag *Fraxinus* was extracted from the FIA database. Once the sample was prepared and irrelevant observations were removed, the resultant sample was composed of 2677 individual *Fraxinus* observations, with 1857 of them being repeat observations from the Northeastern USA. This data was used to train a system of equations to describe the life-cycle of a *Fraxinus* snag as it decays and eventually falls (Forest Inventory and Analysis, 2022). Trees per hectare (TPH) and diameter at breast height (DBH) were used as additional site factors for the spatial model due to the small target region relative to the wide sampling distance of FIA test plots. Due to how the sample data for decay is defined, it was necessary to take a categorical approach as the FIA records the qualitative description of snag condition as listed in Table 1.

Once the trees have fallen, it is expected that a proportion of them will be a hazard by falling on electric distribution infrastructure. The proportion is determined according to their height and their distance from the distribution infrastructure. The basal area per hectare determined from the EAB spread model is split into individual trees based on the size distribution of *Fraxinus* in New Jersey's state inventories (Crocker et al., 2017; Forest Inventory and Analysis, 2022; Woudenberg et al., 2010). The height of the fallen *Fraxinus* is estimated from all *Fraxinus* that have been recorded by the FIA in the Northeastern USA. Also, the height of the sample is related to their DBH, which can be compared with New Jersey's state inventories (Forest Inventory and Analysis, 2022).

Table 1
Summary of decay classes of snag trees from the Forest Inventory Analysis, Department of Forestry.

Decay class	Description (McRoberts et al., 2005)
1 (STA)	All limbs, pointed top, 100% bark, intact sapwood, height intact.
2 (STB)	Few limbs, top may be broken, some bark and height loss, sapwood decay.
3 (STC)	Limb stubs, broken bole, bark and sapwood sloughed, broken top.
4 (STD)	Few stubs, bole broken/rotten, 50% bark, sapwood sloughed.
5 (STE)	No stubs, broken and rotten bole, 20% bark, sapwood gone, rotten 50%.

To estimate the location and length of the relevant electrical distribution infrastructure, we considered the locations of transformers that were submitted for the New Jersey Department of Environmental Protection (NJDEP) Solar Capacity project in 2016 (Bureau of Climate Change and Clean Energy, 2021). Then, we associated the transformer locations with their local road network, as sourced from the USA Census TIGER/line roads database (Bureau of Transportation Statistics et al., 2016). With the transformers associated with their local roads, the point locations were connected by lines according to the road network associations.

Using the estimated number of fallen trees and the distribution network, the number of hazard trees that intersect any distribution infrastructure, along with potential costs, can then be calculated. In doing this, it was assumed that the tree has an equal chance to be in any part of the local forest and have the potential to fall and intersect the distribution infrastructure located there as a function of the amount of infrastructure present. Furthermore, the taller the tree is, the more likely that it could hit the infrastructure, as it can be further away from the infrastructure and still be a hazard when it falls. This damage then has a resultant cost from either preventative maintenance on the hazard tree or repair of the distribution infrastructure.

In sum, our methodology consists of the following seven primary steps, with details of each provided in the following sections: (1) we compute the basal area of dead snags in each location (see Section 2.1); (2) we find the distribution of size classes for different tree sizes (see Section 2.2); (3) we estimate the height of trees in each size class (see Section 2.3); (4) we estimate the transitions between decay classes using categorical methods trained on FIA data, and the results are applied to the EAB-killed *Fraxinus* trees (see Section 2.4); (5) we estimate the length of power lines and poles in the study area using GIS-based transformer location data (see Section 2.5); (6) we find the probability that any one of the falling trees intersects with the distribution infrastructure (see Section 2.6); and (7) we estimate the cost of this intersection either in terms of preventative maintenance, or repairs (see Section 2.7). All codes used in the analysis are available at https://github.com/EWLyttek/Infrastructure_Damage/tree/main.

2.1. *Fraxinus* snag generation

To track the accumulation of snags and the decay of *Fraxinus* in the forest system, the accumulation of snag basal area (BA) in the first decay class is set equal to the consumption of *Fraxinus* by EAB (Eq. (1)) based on the methodology of the EAB spread model developed in Lyttek (2023), and detailed in Appendix A. The core equations for the EAB spread model used in this work are given as

$$\frac{\partial ST_a}{\partial t} = CE_l, \tag{1}$$

$$\frac{\partial A}{\partial t} = \begin{cases} \hat{G}_1 A - \hat{C} F_c A^2 - CE_l & \frac{A}{A_{(1)}} \geq 0.1 F_c \\ \hat{G}_2 A - \hat{C} F_c A^2 - CE_l & \frac{A}{A_{(1)}} < 0.1 F_c, \end{cases} \tag{2}$$

where ST_a is the amount of standing *Fraxinus* snags, which are created at the rate of *Fraxinus* consumption by EAB (C) and the local population of EAB larva (E_l). In Eq. (2), the amount of *Fraxinus* trees (A) do not spread outside their cells and are assumed to grow and regenerate according to the growth rate $\hat{G}_1$ or $\hat{G}_2$, while the population is capped by the crowding rate $\hat{C}$. Note that the choice of growth rate depends on which part of the piecewise-defined equation is used, as determined by the ratio of the amount of *Fraxinus* at time t and the initial amount of *Fraxinus*, given by $A_{(1)}$.

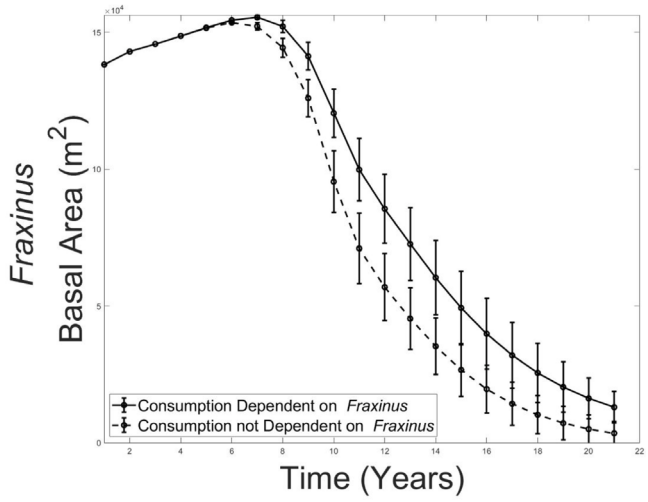

Fig. 1. Comparison of *Fraxinus* basal area in time for different consumption coefficients. The altered consumption coefficient results in a slightly faster decline in Fraxinus as well as a lower end-state when compared to the primary parameterization found in Lyttek et al. 2023 (Lyttek, 2023).

Crowding is modified by F_c, which describes the local canopy cover as an approximation for forest cover (U.S. Geological Survey, 2019). *Fraxinus* is reduced due to consumption by EAB larva at the same rate C constrained only by EAB's biological capacity so that *Fraxinus* decline can be tracked irrespective of EAB's behavior. This is in contrast to the primary parameterization in Lyttek et al. 2023 (Lyttek, 2023), where C is normalized to the population of EAB to examine specifically EAB population dynamics. The readjustment of this type shows limited differences to the baseline as seen in Fig. 1. The comparison shows the difference between these two parameterizations over 16 runs for Essex County, a small county adjacent to the study area that was used for parameterization validation. In particular, one sees a slightly faster decline in *Fraxinus* along with a slightly lower end-state.

This snag generation structure was computed for the three northern New Jersey counties of Morris, Sussex, and Warren, where there is still extant *Fraxinus* at the time of writing.

2.2. Size class distribution estimation

With the calculated BA of snags using the altered EAB spread model in the previous section, the relative proportion of BA that is in each DBH size class of *Fraxinus* in the study area is calculated from state inventories. Ten years (2009–2019) of *Fraxinus* data is used to estimate the proportion of basal area that is associated with each recorded class of DBH size class of *Fraxinus* on forest land in New Jersey (Crocker et al., 2017; Woudenberg et al., 2010; Forest Inventory and Analysis, 2022).

Once the number of trees and basal area of the state divided by the expected size class were compiled and normalized by each size class' individual BA, one obtains the distribution shown in Fig. 2. The

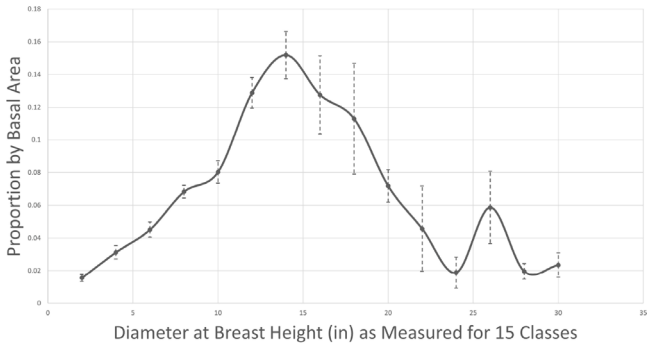

Fig. 2. Variation in the distribution of *Fraxinus* size classes by proportion in New Jersey from 2009–2019.

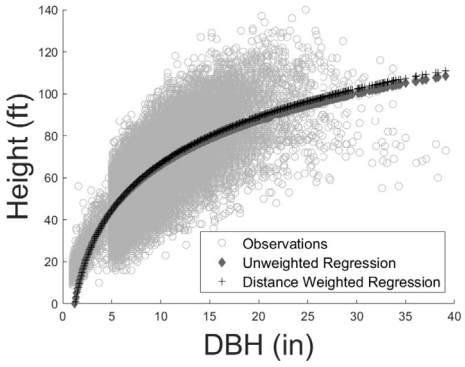

Fig. 3. Distribution of samples and the curve of best fit between DBH and height.

distribution shows that, for example, any unit of BA, approximately 15% will fall into the 14-inch DBH size class. The distribution allows for the assignment of basal area to all size classes of trees according to their relative abundance in the target forests. As trees get larger, they individually contribute more to the BA, but are also significantly rarer and so have a higher sampled error between inventory years that is not seen in smaller specimens.

2.3. *Fraxinus* height regression based on DBH

With the distribution of *Fraxinus* DBH from the previous section, one can estimate tree height relative to tree diameter. The height of *Fraxinus* is dependent on the region being studied. To estimate the height of *Fraxinus* snags, we plotted height versus DBH for over 30,000 live *Fraxinus* trees that were sampled by the FIA from 2000-2020 (Forest Inventory and Analysis, 2022).

This sample was taken from New Jersey and surrounding states, including Pennsylvania, New York, Delaware, and Connecticut (Fig. 3). The data is somewhat disparate with only one explanatory factor, but the fit did not improve upon including other data that could be spatially referenced in the study area. Testing with other recorded parameters, such as site elevation and site conditions, did not provide any additional insight into the height of *Fraxinus*, so without justification for multivariate analysis, DBH was maintained as the sole predictor of height (Fig. 3).

The best fit was found using a log-linear regression for the size of *Fraxinus* in the study area. The fit has a ±9.31 foot error when the samples were weighted based on their distance to the study area. That is, the further the samples were from the geographic center of the study region in Northern New Jersey, the lower the weight they had in the regression. This distance was kept coarse using decimal degrees as the distance, as plot locations and exact distance for the samples are purposefully made imprecise to protect the locations of the FIA plots and prevent tampering (Forest Inventory and Analysis, 2022).

We determined that

$$Ht_{(ft)} = 32.26 \log(DBH_{in}) - 7.37 \quad (3)$$

where $Ht_{(ft)}$ is the height in feet and DBH_{in} is the diameter at breast height in inches. The standard deviation is 10 ft, which is likely explained by site factors with a Mean Squared Error (MSE) of 86.70 and an error parameter of ±9.31. An unweighted distribution performed much worse with a significantly higher MSE of 144.71 (Fig. 3).

Table 2
Transition matrix for decay classes, showing the probability that a tree in a certain class will transition to another decay class or fall by the next resampling period.

Decay class	1	2	3	4	5	Fallen
1	0.028	0.197	0.229	0.020	0.000	0.526
2	0.000	0.164	0.218	0.034	0.002	0.583
3	0.000	0.000	0.173	0.043	0.008	0.776
4	0.000	0.000	0.000	0.096	0.007	0.897
5	0.000	0.000	0.000	0.000	0.030	0.970

2.4. Decay rate and fall chance

The residence time and decay state of Fraxinus snags influence how quickly dead snags fall. With increasing decay, the snag has a higher chance of falling. With the results of the three previous sections, the next step is focused on describing how *Fraxinus* decays through time. The sample period was limited to the years 2000–2020, as earlier data did not thoroughly sample snags, and later data had not been resampled. The sample data was sourced from the same states that were used for height, namely New Jersey, Pennsylvania, New York, Delaware, and Connecticut (Forest Inventory and Analysis, 2022). Once the FIA data had been cleaned of any snag *Fraxinus* that had been artificially removed or otherwise compromised, the data was evaluated using the five FIA decay classes (Table 1).

The sample comprised 2677 individual records, with 1857 of them being repeat observations. When trees are not sampled in the next period it is assumed that the tree has fallen based on FIA sampling protocols (Woudenberg et al., 2010). A small number of samples were noted to revert decay classes on follow-up inspections. However, as it is biologically impossible to become less decayed over time, we assume that *Fraxinus* can only advance decay classes (Table 2). Additionally, we treat inventory resample periods as equivalent for all snag records. The measurement times varied in some cases, and while resampling usually occurred every five years, a small portion was resampled on a four- or six-year timescale. However, the transition matrix is treated as an approximation for a five-year resurvey interval, as that was by far the most common interval with the four- and six-year intervals happening in a minority of cases.

Concatenation of the sample results in a transition matrix of probabilities where trees either stay in their current decay class, or transition to a more advanced state of decay, or fall between sample periods (Table 2). For example, if a tree starts the period in decay class 1, it will have a 0.526 probability of falling by the next resampling period, and a small 0.028 probability of remaining in decay class 1 by the next resampling period. This transition matrix is used to define a Markov Chain process for a system of equations that will be used to define the transition of *Fraxinus* under varying site conditions. The system of equations is trained using a random walk process according to a Markov Chain Monte Carlo process (MCMC). The model is trained in rJAGS and is built out of 15 individual equations (Depaoli et al., 2016; Plummer, 2003).

The system of equations consists of a combination of logistic regression and softmax categorical regression. Logistic regression is often

used for classification into either the 'positive' category or 'negative' category. The logistic function is defined as

$$\sigma(z) = \frac{1}{1 + e^{-(\beta z)}}, \tag{4}$$

where $\sigma(z)$ is the probability of an outcome under condition z, which are believed to relate to the outcome, and β is a trained parameter that weights the impact of condition z. Logistic functions are used to calculate the probability of an event when the output has only two outcomes, as is the case when decay is in the last stage and *Fraxinus* will either fall or remain standing.

Softmax categorical regression is an extension of logistic regression when there are more than two possible outcomes. Since the remaining decay classes have more than two potential states at the next sample period, they are categorized as softmax categorical regressions, defined as

$$\sigma(\mathbf{z})_i = \frac{e^{\beta_i z_i}}{\Sigma_{j=1}^{K} e^{\beta_j z_j}}, \quad i = 1 \dots K, \tag{5}$$

where K is the number of potential output categories, $\mathbf{z} = (z_1, \dots, z_K) \in \mathbb{R}^K$ is the input condition, and β is a trained weight parameter (Wolfe et al., 2017).

Given the small study region and sample of interest, diameter at breast height (DBH) and trees per hectare (TPH) were included as additional site factors. There are a total of three input parameters: (1) the current decay class of the snag (D_{c_n}), which is the response variable; (2) the diameter class of the tree (D_c), which could influence the tree to either remain standing or fall; and (3) the trees per hectare (TPH), which could influence the tree to either remain standing or fall. For both D_c and TPH, the null effect is defined as the average of the sample and any deviation from there is considered the potential influence. The initial amount of trees in the decay class D_{c_1} is defined as the sum of all mortality in each year from the EAB spread model.

When training the model, the focus is on the transition to the next state for a particular sample. Snags decay out of one decay class (n) and into more advanced classes ($n+1, \dots, n+k$), with some small proportion remaining in the initial decay class. Decay out of a class ($D_{c_n(t)}$) and into another decay class ($D_{c_m(t)}$) in the trained model is defined as

$$D_{c_m(t+5)} = D_{c_n(t)} \left(\frac{e^{(\beta D_{c_m} + \beta_1 D_c + \beta_2 TPH)}}{\Sigma_{j=1}^{K} e^{(\beta D_{c_j} + \beta_1 D_c + \beta_2 TPH)}} \right), \tag{6}$$

where D_c is the diameter class of the *Fraxinus* basal area, n is the initial decay class being evaluated, m is the decay class whose transition is being evaluated, t is the initial year, TPH is the trees per hectare in that sample location, K is the number of decay classes, β is the trained parameter for transitioning between decay classes n and m, β_1 is the trained parameter for the influence of size class and β_2 is the trained parameter for the influence of trees per hectare. One can see from Eq. (6) that the amount of *Fraxinus* BA in decay class n that will enter class m at time $t+5$ is proportional to the amount present now according to softmax regression. The structure of the regression is identical for all cases except for decay class 5. Since there are only two potential outcomes for decay class 5, logistic regression is used, but influencing variables remain identical.

The model was trained in rJAGS using the Gibbs sampling algorithm, a variation of the Metropolis–Hastings algorithm for MCMC systems (Depaoli et al., 2016; Plummer, 2003). The model trained across three Markov chains simultaneously, and after a 1000-step burn-in to account for noise in the first steps of the Markov Chains, 20,000 samples were extracted and the mean of the best fit was taken to define the model system.

The process determines the trained weight parameters for each potential transition and site factor. The results showed that in general larger snags are more likely to transition to a more advanced decay class, but are no more likely to fall. The site factor parameters also show that, in general, snags in denser stands are no more likely to transition to a higher decay class, but are less likely to fall. Additionally, for each decay class, there is a far higher probability to transition into the fallen decay class than there is to remain in one of the standing decay classes with large positive numbers for each parameter associated with tree failure. Specific values of β are shown in Table B.6 in Appendix B. The site factors are only displayed in terms of whether they influence the possibility of the specimen falling or remaining standing in order to reduce the number of parameters that need to be trained, due to the limited sample size that could be extracted.

2.5. Distribution infrastructure location and trees per hectare estimation

The final two factors to estimate are (1) the estimated trees per hectare (TPH), as stand density is a significant factor in determining how fast trees fall, and (2) the distribution network for the electric grid which is at risk from tree fall (Hughes et al., 2021; Oberle et al., 2018b). To estimate the TPH, the forest cover percentage (see Eq. (2) and Ref. Lyttek et al. (2019)) is multiplied by 1400. This average value TPH was sourced from a combination of the average of New Jersey State Inventories and the FIA sample data for *Fraxinus* from the entire sample region (Crocker et al., 2017; McRoberts et al., 2005; Forest Inventory and Analysis, 2022).

The length of power lines in each cell where *Fraxinus* is located was estimated by geo-referencing the locations of transformers submitted for the New Jersey Department of Environmental Protection (NJDEP) Solar Capacity project in 2016 (Bureau of Climate Change and Clean Energy, 2021). This report was developed using NJDEP Geographic Information System (GIS) digital data, but this secondary product has not been verified by NJDEP and is not state-authorized or endorsed. The transformers were then referenced to the local road network sourced from the TIGER/line roads database and translated into strings of points to allow for the ordering of transformers along the length of each road (Bureau of Transportation Statistics et al., 2016).

The referenced transformers were then connected to measure the approximate length of the distribution network in the study area (Fig. 4). This approximated distribution network is not perfect information as it does not connect the network across roadway intersections. Further, other mapped distribution networks are not available for the study area, and given the method involved, likely slightly underestimates the actual network. The distribution displayed in Fig. 4 shows significant coverage in the southern and eastern portions of the study area. The height of the distribution network is defined as 35 ft, which is the average height of distribution power lines in the region, but with expected upgrades due to electrification, a height of 60 ft is also considered (Public Service Electric & Gas Co. (PSE&G), 2007; Warwick et al., 2016).

2.6. Modeling fall risk

At this stage, there are five inputs for the model, including (1) the distribution of standing dead *Fraxinus* due to EAB infestation, (2) the height of the standing dead trees, (3) the transition probabilities between the decayed and fallen classes of *Fraxinus*, (4) the estimated length of the local power distribution network, and (5) the height of the distribution. Next a set of equations is constructed to relate the expected proportional fall of *Fraxinus* to spatial data so that

$$D_{c_n x(t+5)} = D_{c_n t} \left(1 - \sum_{m=n+1}^{K} \frac{e^{\beta D_{c_m} + \beta_1 D_c + \beta_2 TPH}}{\Sigma_{j=1}^{K} e^{\beta D_{c_j} + \beta_1 D_c + \beta_2 TPH}} \right), \tag{7}$$

where D_c is the diameter class of the *Fraxinus* basal area, n is the decay class being evaluated, x indicates the amount of *Fraxinus* remaining at $t+5$ from the original amount, m indexes decay classes more advanced than decay class n, t is the year of input data from the EAB spread model being evaluated, TPH is the estimated trees per hectare in that location, K is the number of decay classes, β is the trained parameter

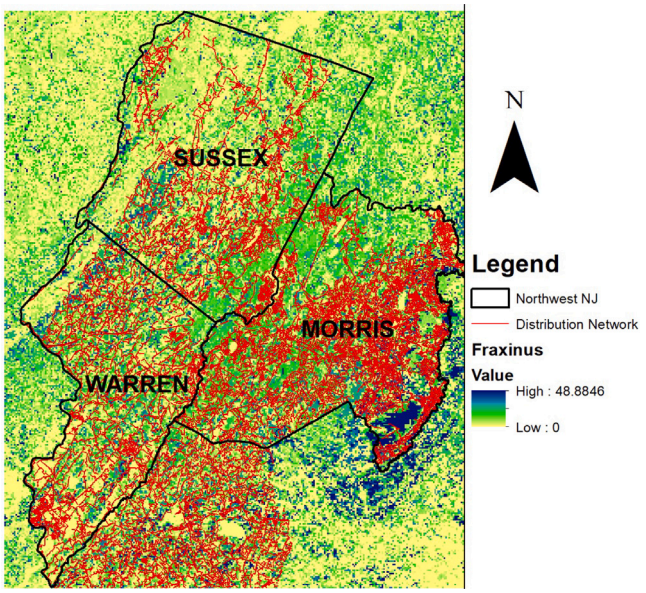

Fig. 4. Map of Northwestern New Jersey showing the location of *Fraxinus* and the electrical distribution infrastructure.

for transitioning between decay classes, β_1 is the trained parameter for the influence of size class, and β_2 is the trained parameter for the influence of trees per hectare. Eq. (7) shows that the amount of *Fraxinus* BA in decay class n at time $t + 5$ is equal to the amount present now multiplied by the difference of unity and the sum of the proportions of BA in decay class n at time t that are advancing to a more advanced decay class.

Any classes in less advanced states of decay will feed into the system adding material to the decay class n so that

$$D_{c_n(t+5)} = D_{c_n x(t+5)} + \sum_{m=1}^{n-1} D_{c_m(t)} \frac{e^{\beta D_{c_m} + \beta_1 D_c + \beta_2 TPH}}{\Sigma_{j=1}^{K} e^{\beta D_{c_j} + \beta_1 D_c + \beta_2 TPH}}. \quad (8)$$

All terms in Eq. (8) are the same as in Eq. (7), except now m is indexing decay classes less advanced than decay class n. Overall, Eq. (8) shows that part of each decay class m at time t transitions into decay class n at $t + 5$.

Transitions into the fallen class were found based on the transition from each decay class to the fallen class, stored by year and diameter class, so that

$$D_{c_f(t+5)} = \sum_{n=1}^{f-1} D_{c_n(t)} \frac{e^{\beta D_{c_f} + \beta_1 D_c + \beta_2 TPH}}{\Sigma_{j=1}^{K} e^{\beta D_{c_j} + \beta_1 D_c + \beta_2 TPH}}. \quad (9)$$

Eq. (9) shows that the fallen class in the next period equals the sum that falls from each standing decay class. This system of equations is used to process all the spatial data for the study area for 40 years using the EAB spread model. We chose 40 years as the time-frame for the model as this time period allows an additional 20 years beyond the end of the EAB model's computation for the decay and fall of *Fraxinus* that were affected in the final year of the EAB spread model.

After snag fall has been projected, the next step is to determine which snags could cause damage to distribution infrastructure. The predicted *Fraxinus* mortality is combined with the length of the electric lines present to estimate the number of *Fraxinus* that will probabilistically fall on the electric lines. The topographical relationship between *Fraxinus* snags and infrastructure assumes that on average, equal numbers of trees will be on level terrain compared to the distribution infrastructure. Therefore, topography is not considered in the height calculations.

The probability of a tree falling towards or away from the distribution infrastructure is set as a binary outcome, as further detailed probabilities would require specific knowledge of the conditions around the distribution infrastructure. No-risk cases, where the distribution infrastructure is taller than the potential hazard tree, are not evaluated.

To calculate the number of potential hazard trees, the ratio of basal area in a size class (D_c) over the basal area of one tree in that size class (BA_c) is calculated. The number of fallen trees that impact distribution infrastructure is defined as a proportion of the area P that contains both hazard *Fraxinus*, $\frac{D_{c(t)}}{BA_c}$, and length of distribution lines, G_l, combined with the distance from distribution infrastructure which *Fraxinus* of a certain height can be, D_g.

To define the distance, D_g, the height of the distribution grid, H_g, and the height of the tree, H_t are used. These two heights form two legs of a right triangle when the average slope between the *Fraxinus* snag and distribution infrastructure is assumed to be zero. The Pythagorean theorem is utilized to solve for the distance between the pole and the tree such that the tree forms the hypotenuse.

Taken together, this relationship is defined as

$$F_{r_c} = \begin{cases} 0 & H_c < H_g, \\ 0.5 \left(\frac{D_{c(t)}}{BA_c} \cdot \frac{\left(G_l \sqrt{H_c^2 - H_G^2}\right)}{P} \right) & H_c > H_g, \end{cases} \quad (10)$$

where F_{r_c} is the number of trees falling on distribution infrastructure for a size class of trees, 0.5 is the random chance that a tree in the danger area falls towards the infrastructure, $D_{c(t)}$ is the basal area that has fallen in one size class, BA_c is the average basal area per tree in each size class (so that the ratio $\frac{Dc(t)}{BA_c}$ defines the number of trees in size class c at time t), G_l is the length in meters of the local electric lines, H_c is the height of diameter class c, H_g is the height of the electric lines and P is the area of a pixel, which in this work is a square hectare.

2.7. Economic costs of treefall

The costs in 2022 dollars for a tree falling on a power line are counted as a direct cost between $4,508 and $13,518, with an average of $7,574, based on the cost for a new mile of traditional overhead power lines and the assumption that the damage compromises the line between two utility poles, usually a length of between 100 and 300 ft depending on site conditions (Warwick et al., 2016). This cost does not consider overtime, or the urgency of the remedial work.

The cost in 2022 dollars of removing a tree is set between $1,166 and $3,499, with an average of $1,960, for normal operations and management of tree removal. Precise estimates are not available for the cost of tree removal due to the nature of the work. This cost has therefore been determined from local contractors' estimation (Amazing Tree Services, 2017; Moosewood Tree Service, 2017).

In the case of line repair and tree removal, costs are assumed to approach the low end of the presented ranges due to economies of scale and to not overstate the issue. The cost of the upgrade is significant at approximately $238,000 per mile ($147.88 per meter), but will likely be done at some point in the future regardless, due to increasing electrification of the state (Public Service Electric & Gas Co. (PSE&G), 2007; Warwick et al., 2016). This means that decreased incidence of costly treefall events, given a 15-foot higher line height, is an ancillary benefit of a policy that is already being enacted. A discount rate of 3 percent was employed as

$$C_t = \frac{(F_r * C_s)}{1.03^t}, \quad (11)$$

where C_s is the estimated economic costs of the system, and F_r, is the number of incident trees. Eq. (11) allows one to account for the time since the initial fall and to calculate the present value of either the removal, or topping, of incident trees with the current, or upgraded infrastructure in a given year, t. These costs are then summed over the total number of years, T. Costs were computed at the site level and then compiled for the entire study area to provide an estimate for both the total cost, as well as average site conditions.

3. Results

The diffusion-based PDE model described in Section 2.1 is used to track the spread of EAB and the subsequent decline of *Fraxinus* population in time throughout the study region. The resultant *Fraxinus* mortality information is used to determine the location of snags that have the potential to impact nearby infrastructure. These snags will decay through time, where the decay is measured using the five decay states as classified by the FIA (Forest Inventory and Analysis, 2022). We then use regression modeling to compute the probabilities of moving from one decay class to another decay class (see Section 2.4).

To examine this modeling structure and the potential outcomes, we considered a set of 10 scenarios, labeled S1-S10. Scenarios S1-S5 disregard the spatial distribution of snags in time which is found using the PDE model, and instead examine the potential costs due to a specified *Fraxinus* distribution at different times. Scenarios S6-S10 integrate the PDE model in the computations and examine the impacts of *Fraxinus* growth under different EAB introduction and spread patterns.

Our results show the importance of spatial simulation and forecasting of EAB spread to determine the costs of EAB-induced *Fraxinus* snags on the electrical grid. When all vulnerable *Fraxinus* trees die immediately upon the introduction of EAB (year one mortality) and begin to decay (decay class 1), the result is high costs to the utility for the current grid with no mitigation via tree topping or trimming (Table 3, Scenario S1, Column 3).

When these costs are graphed over time (Fig. 5), a stepping pattern emerges due to the FIA's 5-year resampling period (Forest Inventory and Analysis, 2022). The error associated with the current grid with no mitigation is ±30% due to the uncertainty when estimating the heights of trees over a large area (see Section 2.2 and Section 2.3). Other factors, including the variability in *Fraxinus* fall rates (Table 3, Scenario S1 versus Scenarios S2 & S3), result in far less variability (figure not shown).

Despite the uncertainty from tree height estimation, the impacts to the unmitigated current distribution infrastructure (Table 3, all scenarios, Column 3) are decidedly higher than when the infrastructure has been upgraded to meet the 69 kV initiative goals (Public Service Electric & Gas Co. (PSE&G), 2007) (Table 3, all scenarios, Column 4). Moreover, while the upgrade of the infrastructure reduces costs from *Fraxinus* snags significantly, the most effective method is to mitigate the threat by identifying and removing all potentially dangerous trees near the distribution lines (Table 3, all scenarios, Column 5 and 6).

The magnitude of these costs is also significantly impacted by how aggressively future costs are discounted. In particular, if *Fraxinus* mortality is entirely delayed by 20 years, and if discounting is kept at a moderate 3%, then the impact of snags is approximately halved when compared to scenarios S1-S3 (Table 3, Scenario S4). Once mortality is spread over multiple years, as in Scenario S5, it smooths the cost curve (Fig. 6). However, the overall result is similar, with discounting not making a large difference in the total cost. This reinforces the result of scenario S4 in that the timing of *Fraxinus* mortality influences costs if there is a long enough lag.

When one views the costs in each scenario as a function of time (Figs. 5 and 6 for scenarios S1 and S5 respectively), it becomes apparent that the costs are largely incurred in the first few years after *Fraxinus* mortality occurs. Scenario S1 shows a strong stepping pattern as all snag-falls are updated in the same year, with almost half of the costs already incurred only five years after *Fraxinus* are assumed to become snags (Fig. 5). Scenario S5 is similar but the cost curve is much smoother due to the mortality occurring over a five year period (Fig. 6).

Scenarios S1-S5 provide a baseline estimate. Scenarios S6-S10 provide estimates using the more realistic EAB spread model for different initial spatial patterns of EAB introduction (see Appendix A). Because *Fraxinus* growth over the course of the EAB infestation is included in the EAB spread model, much higher costs are incurred for scenarios S6-S9 when compared to the fixed introduction scenarios S1-S5.

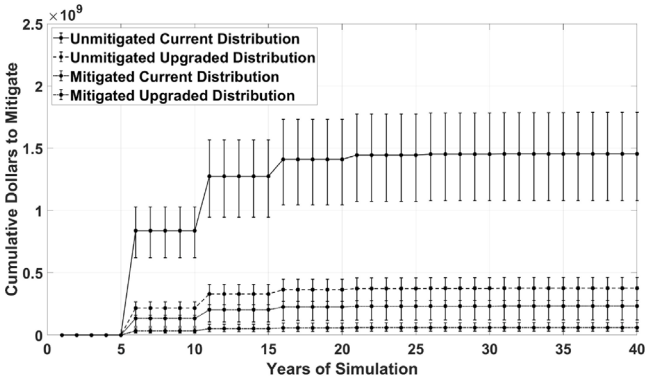

Fig. 5. Cumulative costs associated with scenario S1. All trees currently in place are assumed to fail in year 1 and immediately begin to decay. Because of the FIA resampling period, the damages due to snag fall are updated every fifth year. Mitigation assumes that all *Fraxinus* are removed before snag fall occurs, thus avoiding repair costs.

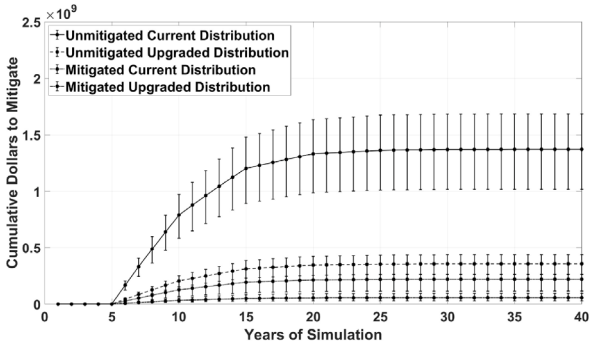

Fig. 6. Cumulative costs associated with scenario S5. Mortality of trees is staggered evenly over a five-year period, which results in a smoother cost curve when compared with the immediate mortality in the year 1 scenario (Scenario S1).

The growth of *Fraxinus* over the course of the EAB infestation outpaces discounting of future costs significantly, despite mass mortality of *Fraxinus* occurring in years 12-13 of the simulated EAB infestation. The greater magnitude of the result is caused by the aggressive regrowth and sprouting that is a feature of the EAB model for damaged *Fraxinus* (Fig. 7). All four scenarios (S6-S9) have very similar costs, which shows that damages are not highly dependent on the initial random distribution of EAB.

In Scenario S10, *Fraxinus* regrowth is not allowed. Instead, *Fraxinus* is only allowed to grow at a rate commensurate with mature trees (Schlesinger, 1990), thus leading to overall lower costs. This variation on the scenario S6-S9 enables one to assess the effect that new growth from recently EAB-killed stands of *Fraxinus* has on the results. Although there is a decrease in cost associated with scenario S10 compared with scenarios S6-S9, in reality the regrowth from stump sprouts and the seed bank would not be a significant risk to infrastructure since all resulting *Fraxinus* would be sapling-sized for the foreseeable future, and thus too small to be of concern (Table 3 and Fig. 8).

Given the amounts described in Table 3, it is important to understand how these total costs relate to the estimated 9,800 kilometers of electric distribution lines in the study area. Additionally, it is important to understand how this relationship could influence policy decisions. Based on economic costs, repairs across an individual hectare-sized site within the study area can range from $0 to $406,000. Because of the wide range of repair costs, we have investigated which conditions are

Table 3
Summary of the amount of damage incurred by *Fraxinus* snag fall in millions of 2022 dollars. The highest estimates occur when incident trees impact the existing grid with no mitigation via topping or trimming of trees (Column 3). Other estimates are associated with the upgraded grid and no mitigation (Column 4), the current grid with mitigation (Column 5), and the upgraded grid with mitigation (Column 6). Scenarios S1-S3 consider the current *Fraxinus* distribution all dying in year 1 with different snag fall rates, while scenarios S4 and S5 consider respectively delayed mortality or mortality spread evenly over a period of time. Scenarios S6-S9 use *Fraxinus* mortality as determined by the EAB spread model with different random introductions of EAB into the region. Scenario S10 is the same as scenario S8, but does not allow *Fraxinus* to regrow quickly after infestation.

Scenario	Description	Unmitigated current distribution	Unmitigated upgraded distribution	Mitigated current distribution	Mitigated upgraded distribution
S1: Immediate Mortality in Year 1	All *Fraxinus* present in the survey fails in year 1 and begins to decay.	$1,455	$376	$233	$60
S2: Immediate Mortality in Year 1 With Slower Snag Fall Rates	Same as S1, but with decreased snag fall rates.	$1,443	$373	$231	$60
S3: Immediate Mortality in Year 1 With Faster Snag Fall Rates	Same as S1, but with increased snag fall rates.	$1,461	$378	$235	$61
S4: Immediate Mortality in Year 20	All *Fraxinus* mortality is delayed until year 20.	$829	$215	$133	$34
S5: Mortality Occurs Evenly Over Five Years	All *Fraxinus* mortality occurs evenly over a 5 year span, with no regrowth.	$1,372	$354	$220	$57
S6: Realization 1 Of The EAB Spread Model	Mortality determined using EAB model, with random EAB introduction Pattern 1.	$1,937	$501	$311	$80
S7: Realization 2 Of The EAB Spread Model	Mortality determined using EAB model, with random EAB introduction Pattern 2.	$1,945	$503	$312	$81
S8: Realization 3 Of The EAB Spread Model	Mortality determined using EAB model, with random EAB introduction Pattern 3.	$1,945	$503	$312	$81
S9: Realization 4 Of The EAB Spread Model	Mortality determined using EAB model, with random EAB introduction Pattern 4.	$1,945	$503	$312	$81
S10: Realization 3 Of The EAB Spread Model, With No Regrowth	S8, with no regrowth of *Fraxinus*.	$1,798	$465	$288	$75

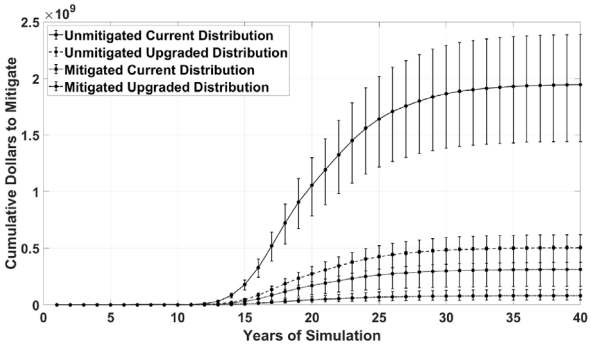

Fig. 7. Cumulative costs associated with scenario S8. The spread of EAB with a regrowth *Fraxinus* results in a dramatic increase of *Fraxinus* mortality in year 13, leading to a steep cost curve. As *Fraxinus* regrows the cost continues to rise over the intervening years leading to inflated costs over the course of the study.

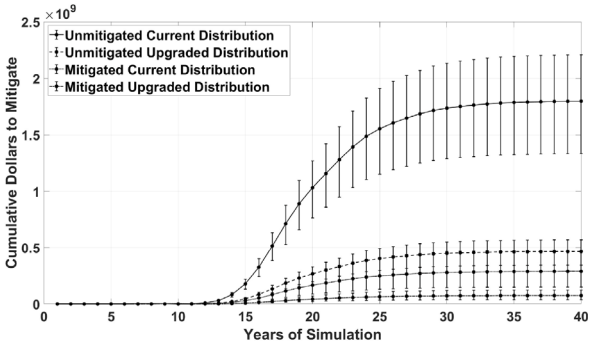

Fig. 8. Cumulative costs associated with scenario S10. The spread of EAB results in an increase of *Fraxinus* mortality after 13 years, thus leading to a steep cost curve. However, without aggressive sprouting and regrowth, there is a much lower peak in costs. This scenario shows costs with a reduction of approximately $150 million when compared with scenarios S6-S9.

most responsible for affecting the level of cost. Through a comprehensive study of all input variables, we have determined that the total cost is most strongly related with the product of the length of electric distribution lines in meters and the basal area of *Fraxinus* present in the study area (Fig. 9). The linear trend seen in Fig. 9 is observed across all scenarios S1-S10, but the slope of the trend line is influenced by the treatment cost employed in each scenario. Fig. 10 shows that the spatial distribution of the high-damage points is more easterly in distribution. The positive relationship between these factors is expected. However, given the large number of highly varied input variables, it is somewhat surprising that two factors alone are the primary driver for determining the cost.

We have previously discussed the upgrade of the electric distribution and have described the significant savings associated with an upgraded network, with and without mitigation, for various scenarios. Now we discuss how these savings compare in the context of the electrical distribution infrastructure. Based on the average upgrade cost in 2022 dollars (Warwick et al., 2016), the savings will have to exceed $147.88 per meter of electric grid present (see Section 2.7) in order to match the upgrade cost of the electrical infrastructure.

In scenarios S1-S5, which do not incorporate the growth of *Fraxinus*, the cost benefit (difference between current and upgraded distribution in Table 4) does not come close to matching the average upgrade

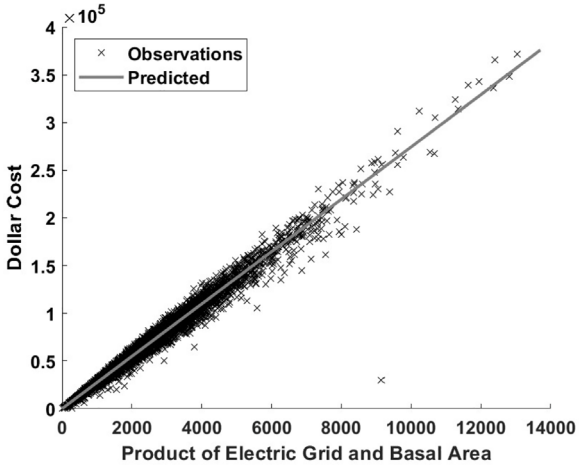

Fig. 9. Relationship between the dollar cost and the input product of length of electric distribution lines and basal area for scenario S8 using the current distribution with mitigation. By plotting the cost versus the product described above for every point in the study area where both *Fraxinus* and electric lines are present, one sees a strongly linear relationship with varying slopes which depend on the specific scenario's cost parameterization.

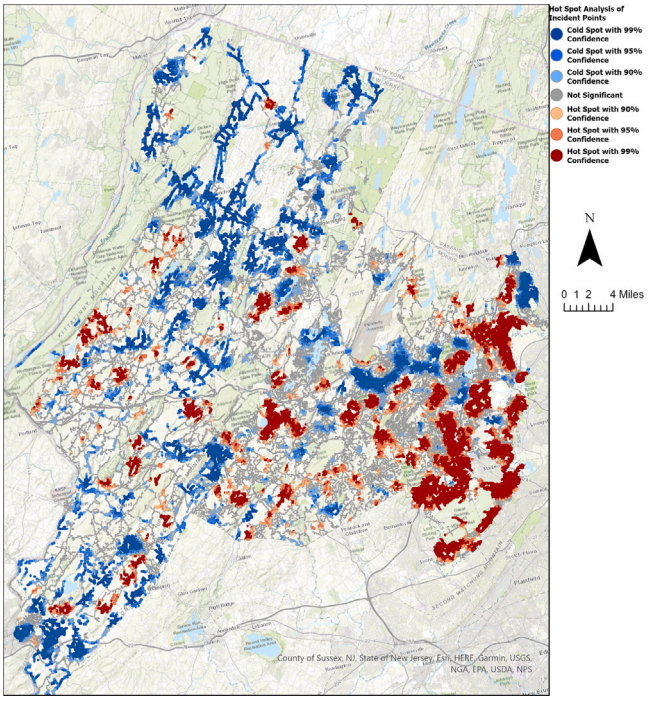

Fig. 10. Map of Northwestern New Jersey showing the location of "hot-spots" of incidence between *Fraxinus* and distribution infrastructure. The map shows a strong clustering of high damage sites to the East of the study area.

cost, even in the case of no mitigation. In particular, the benefit is approximately $110 for scenarios S1, S2, S3, and S5, and approximately $63 for scenario S4.

In scenarios S6-S9, which do incorporate *Fraxinus* growth in the computations, the cost benefit in the unmitigated case is similar to the costs associated with upgrading the distribution infrastructure across the study area. Without line maintenance, the average cost per meter for the current electric distribution infrastructure is just over $190, which decreases to just over $50 for the upgraded infrastructure. In this case, an average of just over $140 of benefits are achieved by upgrading the infrastructure, coming within $10 of the cost benefit (difference between current and upgraded distribution in Table 4). Scenario S10, where regrowth of *Fraxinus* is discounted, exhibits a slight decline in overall costs, but the cost benefit remains approximately $10 for the unmitigated case.

However, if the trees are trimmed, the benefit to upgrading infrastructure is much lower, with approximately $10-$20 of avoided cost (depending on the scenario) per meter of power lines at an average site. This potential savings is significantly below the $147.88 electrical infrastructure upgrade cost and indicates that far less of the planned upgrades are justified by incident snags if the lines are properly maintained. Nevertheless, if line maintenance is not adequate, the scenarios S6-S10 certainly exhibit benefits that would cover a large portion of the incurred costs, which supports the continuation of the 69 kV initiative in New Jersey.

4. Discussion

The presence of EAB-induced dead Fraxinus increases the possibility of grid failure and adverse economic impact on society, and is, therefore, a pressing economic issue for both man-made and natural environments. An integrated ecological-economic understanding can assist in informed decision-making. We have presented a novel method of estimating infrastructure impacts from a forest mortality event, which could be exceptionally useful given the continued prevalence of global trade and the likelihood of similar disturbances to the forest in the future. The method is general, and can be extended to other regions and tree species. One could easily include additional geospatial aspects to forecast a variety of potential risks to vulnerable infrastructure installations.

With regards to the specific example of *Fraxinus* and EAB that we have considered, estimating the costs to infrastructure from a large-scale forest mortality event very much depends on the timing of the mortality event, due to the potential for regrowth of trees which have died. In our computations, different scenarios considered different timings with and without regrowth. The results showed marked differences for these different choices. While the benefit of upgrading distribution infrastructure is not fully compensated by the incidence of *Fraxinus*, if there are upgrades to address capacity issues, the cost benefit will cover much of the cost at an average location, and even more so in some areas.

The methodology for *Fraxinus* snag fall (see Section 2) was particularly enlightening with respect to the degree of damage that EAB is capable of, and enables the identification of locations of special concern. Costs, with current parameterization, are excessive for some locations, with the cost associated with *Fraxinus* management greater than the cost to upgrade to a taller more robust grid, though in most cases the issue was better served by standard line management practices if they are completed in time. With the mortality and decay of *Fraxinus* continuing apace, there is a significant impetus for a detailed survey of electric distribution lines to prevent outages. The model has demonstrated when and where these costs occur, and serves as a framework to evaluate costs across a wide spatial area.

Our methodology is limited only by data uncertainty, namely the height of the target tree species, *Fraxinus*, and the cost estimates for repair of the distribution infrastructure. If precise plot locations for the FIA samples could be obtained for a future study, then improvements to fine-tune the height regression could be accomplished for this example, and for other cases. Machine learning with LiDAR data has been shown to be an efficient solution for this data gap and could bring some definition to the problem involved if precise FIA data can be used as an input (Wang et al., 2021). This extension could also improve knowledge of the general distribution and structure of *Fraxinus* in the forest, allowing even greater accuracy for this study, and for providing a unified method in the future. The repair and distribution estimates can be improved with input from stakeholders in the field, either through surveys or further direct discussion.

Table 4
Summary of the average cost per meter of distribution infrastructure by treatment in 2022 dollars. Columns 2 and 3 shows the costs incurred when *Fraxinus* trees fall on the current or the upgraded network respectively, while columns 4 and 5 shows the costs associated with *Fraxinus* mitigation efforts for the current or the upgraded network respectively.

Scenario	Unmitigated current distribution	Unmitigated upgraded distribution	Mitigated current distribution	Mitigated upgraded distribution
S1: Immediate Mortality in Year 1	$148.26	$38.35	$23.79	$6.15
S2: Immediate Mortality in Year 1 With Slower Snag Fall Rates	$147.04	$38.03	$23.51	$6.08
S3: Immediate Mortality in Year 1 With Faster Snag Fall Rates	$148.94	$38.52	$23.93	$6.19
S4: Immediate Mortality in Year 20	$84.55	$21.87	$13.56	$3.51
S5: Mortality Occurs Evenly Over Five Years	$139.87	$36.18	$22.44	$5.80
S6: Realization 1 Of The EAB Spread Model	$197.43	$51.07	$31.70	$8.20
S7: Realization 2 Of The EAB Spread Model	$198.24	$51.28	$31.83	$8.23
S8: Realization 3 Of The EAB Spread Model	$198.24	$51.28	$31.83	$8.23
S9: Realization 4 Of The EAB Spread Model	$198.24	$51.28	$31.83	$8.23
S10: Realization 3 Of The EAB Spread Model, With No Regrowth	$183.27	$47.40	$29.41	$7.61

5. Conclusion

The widescale mortality of canopy species poses a multitude of negative externalities to the ecosystem, the community, and nearby infrastructure, including electric distribution lines. The resulting snag trees can cause significant damage to critical infrastructure, which needs to be hardened by the neighboring communities and resident utilities, either through tree removals, infrastructure upgrades, or accepting repair costs. Some of these potential measures are more physically effective and have more long-term benefits over time than others. However, this effectiveness is moderated by the variability and uncertainty involved in snag fall rates and snag heights due to forest heterogeneity.

Snag issues caused by the influx of EAB have impacted the electrical grid and will continue to do so until either peak mortality of *Fraxinus* has concluded and *Fraxinus* have been extirpated from the overstory, or the control methods for containing EAB become effective enough to maintain *Fraxinus*. The former case is by far the more likely case, given historical trends, so utilities in the affected regions will need to plan for ways to respond to increased snag incidence and plan for infrastructure maintenance or improvement to mitigate the damages for the foreseeable future.

That said, communities and utilities should realize several factors regarding their planned or projected mitigation. Substantial costs to the grid occur primarily in the first few years after snags appear. Overwhelmingly, the largest share of snag fall incidents takes place within the first five years after mortality, leading to extensive initial costs, with decaying costs beyond that timeframe. If communities and utilities adapt earlier rather than later, the cost-benefit should be in their favor. The strategy that statistically had the best result over time was identifying and removing all potentially dangerous trees in a timely manner along all extent power lines. This figure is likely somewhat understated, as incidental non *Fraxinus* maintenance is not included in the analysis. Having to rely on extensive line maintenance can be problematic for some communities as it is a manpower-intensive strategy with relatively few customers that will be compromised.

However, by all scenarios simulated with available information, the costliest strategy for the utilities regarding EAB-induced snag is to do nothing. Without planning for mitigation and/or infrastructure improvements, the electrical distribution lines and the local community will be negatively impacted due to frequent interruptions and electrical issues. How negatively impacted depends on a variety of conditions including the height of the trees, the height of the infrastructure, the age of the infrastructure, and the density of the surrounding forest. Conditions that can be controlled and minimized will in turn minimize long-term costs associated with the damage caused by EAB. Maintaining infrastructural integrity, especially in the light of extensive electrification efforts by the State, will become pressing as the recently killed *Fraxinus* age and fall.

CRediT authorship contribution statement

Erik Lyttek: Conceptualization, Data curation, Formal analysis, Investigation, Methodology, Project administration, Resources, Software, Validation, Visualization, Writing – original draft, Writing – review & editing. **Pankaj Lal:** Funding acquisition, Methodology, Supervision, Writing – original draft, Writing – review & editing. **Brad Oberle:** Conceptualization, Data curation, Formal analysis, Investigation, Software, Validation, Writing – original draft, Writing – review & editing. **Ram S. Dubey:** Conceptualization, Methodology, Supervision, Writing – original draft, Writing – review & editing. **Eric Forgoston:** Methodology, Software, Supervision, Validation, Writing – original draft, Writing – review & editing.

Declaration of competing interest

The authors declare that they have no known competing financial interests or personal relationships that could have appeared to influence the work reported in this paper.

Data availability

We have included an archived github link to the codes and data used excepting some of the larger raw datasets from the FIA, which can be made available upon request.

Acknowledgments

The authors gratefully acknowledge the support of the Clean Energy and Sustainability Analytics Center at Montclair State University. This research was partially funded by the National Science Foundation Award, USA 1555123. Any opinions, findings, conclusions, or recommendations expressed in this material are those of the authors and do not reflect the views of Montclair State University or the National Science Foundation.

Appendix A. EAB spread model

For completeness, in this appendix we provide an overview of the EAB spread model which tracks both the spread of EAB and the change in *Fraxinus* in time and across a spatial region of interest. In this work, the spread of EAB is simulated for a period of 20 years (T), where each year has 12 constituent months (t). The study period was set to 20 years to account for the historical spread of EAB within a region once it has been infested, but before it enters an endemic state (Poland et al., 2015; Siegert et al., 2014). Meters are the unit of distance, where locations are defined as 100-meter squares ($hs = 100m$). Each of these locations (hs) thus represents a square hectare (ha) and are organized in a grid structure covering the study area. The study area is bounded by a band of null locations to create a regular rectangular grid and to prevent EAB

diffusion through the boundary of the study area. Hectares were chosen as the spatial unit based on Wilson et al. (2012), where BA was tracked in terms of per hectare. EAB are tracked in the x and y dimensions as they diffuse between locations and cause damage to *Fraxinus*.

A.1. EAB-Fraxinus reaction diffusion model

EAB has an active season during which EAB spreads, reproduces, dies, and consumes *Fraxinus* phloem, and an off-season where EAB lies dormant. To simulate this environment the EAB-*Fraxinus* reaction diffusion system has been derived in a piecewise manner. First, in the active on-season, the adult EAB diffusion equation with random introductions takes the form

$$\frac{\partial E_a}{\partial t} = D_u A_s \left(\frac{\partial^2 E_a}{\partial x^2} + \frac{\partial^2 E_a}{\partial y^2} \right) - \Omega E_a + RL, \tag{12}$$

where E_a is the local adult EAB population and $\frac{\partial E_a}{\partial t}$ is the change in EAB adults with respect to time, D_u is the diffusion coefficient, A_s is the stress/abundance coefficient that impacts the spread rate of EAB based on the *Fraxinus* density and damage, Ω is a mortality coefficient for adult EAB, and R and L are the risk factor variables where two randomly generated vectors at a set percentage are compounded to make a low number of additional infestations every year.

On-season growth of EAB larva is modeled as

$$E_l(t_i) = E_l(t_i) + \min(\bar{G}E_a(t_i), \bar{C}A(t_i) - E_l(t_i)), \tag{13}$$

where $E_l(t_i)$ is the larval population at time t_i. The EAB larval population is influenced by the minimum of either the growth function $\bar{G}E_a(t_i)$, or the crowding function, $\bar{C}A(t_i) - E_l(t_i)$. The growth function is the combination between the growth term $\bar{G}$ and the local population of EAB adults $E_a(t_i)$. The crowding function is defined by the crowding $\bar{C}$, and the basal area of *Fraxinus* $A(t_i)$. This equation assumes that all growth happens at the beginning of a time step and that mortality of EAB larva is a smooth curve in time. Then the on-season larval change can be defined as the continuous equation

$$\frac{\partial E_l}{\partial t} = -\omega E_l, \tag{14}$$

where ω is the death rate.

Fraxinus growth in the presence of EAB during the on-season is defined as

$$\frac{\partial A}{\partial t} = \begin{cases} \hat{G}_1 A - \hat{C} F_c A^2 - C E_l A & \frac{A}{A_{(1)}} \geq 0.1 F_c, \\ \hat{G}_2 A - \hat{C} F_c A^2 - C E_l A & \frac{A}{A_{(1)}} < 0.1 F_c, \end{cases} \tag{15}$$

where A is the local population of *Fraxinus* represented as square meters of basal area, $\frac{\partial A}{\partial t}$ is the change in *Fraxinus* with respect to time, $\hat{G}_1$ and $\hat{G}_2$ are the growth rates for *Fraxinus*, $\hat{C}$ is the crowding rate for *Fraxinus*, F_c is the forest cover, C is the consumption rate of EAB larva, and E_l is the population of EAB larva.

The change in off-season larva is set to zero due to the biological fact that they are overwintering and are not undergoing outside stresses. This is also because our growth and crowding factors are based on the average emergence and expansion of EAB, so overwinter mortality is implicit. Therefore

$$\frac{\partial E_l}{\partial t} = 0. \tag{16}$$

Off-season adult EAB are removed from the system, and thus during the off-season the amount of adult EAB is zero so that

$$E_a = 0. \tag{17}$$

Fraxinus growth in the absence of EAB during the off-season is the same as in the on-season, except that there is no consumption by EAB larva and is thus represented by the simplified equation

$$\frac{\partial A}{\partial t} = \begin{cases} \hat{G}_1 A - \hat{C} F_c A^2 & \frac{A}{A_{(1)}} \geq 0.1 F_c \\ \hat{G}_2 A - \hat{C} F_c A^2 & \frac{A}{A_{(1)}} < 0.1 F_c \end{cases} \tag{18}$$

At the beginning of the new on-season, the graduation function sets the number of EAB adults to the number of EAB larva so that

$$E_a \frac{t_0}{T_{i+1}} = E_l \frac{t_{12}}{T_i}. \tag{19}$$

Table A.5 provides a summary of the different model parameters. Further detail regarding the model derivation and parameterization can be found in Ref. Lyttek (2023).

Appendix B. Trained beta values for softmax and logistic regressions

After training the model, the results showed that in general, larger snags are more likely to transition to a more advanced decay class, with a beta.DBHs significantly greater than zero, but are no more likely to fall. The site factor parameters show that in general larger snags are more likely to transition to a more advanced decay class, with a beta.DBHs significantly greater than zero, but are no more likely to fall (beta.DBHf). Snags in denser stands are no more likely to transition to a higher decay class (beta.TPHs) but are less likely to fall, as beta.TPHf is significantly less than zero. Additionally, for each decay class, there was a far higher probability to transition into the fallen decay class than there was to remain in one of the standing decay classes with large positive numbers for each parameter associated with tree failure (Table B.6: beta.1f, beta.2f, beta.3f, beta.4f, and beta.5f).

Table A.5
Summary of parameters for the EAB-*Fraxinus* spread model.

Parameter	Name	Units	Source
T	Years	Year	Poland et al. (2015)
t	Time in Months	$\frac{\text{Month}}{\text{Year}}$	Poland et al. (2015)
hs	Distance between cell locations	m	Wilson et al. (2012)
x	x-axis distance	m	No Source
y	y-axis distance	m	No Source
C	Consumption by EAB	$\frac{\text{ha}}{\text{in}_l\text{t}}$	McCullough and Siegert (2007)
$\hat{G}_{1-2}$	Fraxinus Growth	$\frac{1}{\text{t}}$	Schlesinger (1990)
$\hat{C}$	*Fraxinus* Crowding	$\frac{\text{ha}}{\text{m}^2\text{t}}$	Gould et al. (2020)
F_c	Forest Cover	Percent	U.S. Geological Survey (2019)
A	*Fraxinus* Density	$\frac{\text{BA}}{\text{ha}}$	Wilson et al. (2012)
D	Diffusion Rate	$\frac{\text{m}}{\text{t}}$	Mercader et al. (2009), Siegert et al. (2010)
D_u	Diffusion Coefficient	$\frac{\text{m}^2}{\text{t}}$	Mercader et al. (2009), Siegert et al. (2010)
A_b	*Fraxinus* Relative Abundance Factor	*Unitless*	Siegert et al. (2010), Mercader et al. (2009)
A_{sf}	*Fraxinus* Stress Factor	*Unitless*	Mercader et al. (2011, 2009)
A_s	*Fraxinus*-EAB Diffusion Influence Factor	$\frac{A_b}{A_{sf}}$	Mercader et al. (2009), Siegert et al. (2010), Mercader et al. (2011)

(continued on next page)

Table A.5 (*continued*).

Parameter	Name	Units	Source
E_a	EAB Adult Density	$\frac{in}{ha}$	Poland et al. (2015)
E_l	EAB Larval Density	$\frac{in}{ha}$	Poland et al. (2015)
$\bar{G}$	EAB Growth	$\frac{in_l}{in_a \cdot t}$	Mercader et al. (2016), McCullough and Siegert (2007)
$\bar{C}$	EAB Crowding	$\frac{in}{m^2 BA}$	Duan et al. (2013), McCullough and Siegert (2007)
R	Risk Vector	Binary	Mercader et al. (2016), Ali et al. (2015), Siegert et al. (2014)
L	Adult Introduction Rate	$\frac{E_a}{t}$	Siegert et al. (2014)
RL	Risk of New Infestation	Percent	Siegert et al. (2015, 2014)
ω	EAB Death Rate	$\frac{1}{t}$	No Source, Test Variable

Table B.6
Selected beta values for the transition of *Fraxinus* between decay classes with associated uncertainty measurements of standard deviation, naïve standard error, and time-series standard Error. Standard error indicates the uncertainty in the beta values due to variability in the data set, while naïve/time-Series errors indicate uncertainty from the MCMC training process. In this case, both naïve and time-series errors are much less than the standard deviation, indicating model convergence (Depaoli et al., 2016; Plummer, 2003). Scenarios S2 and S3 use the standard deviation to test for variance in model results rather than the smaller MCMC error values.

Beta	Mean	Standard deviation	Naïve standard error	Time-series standard error
beta.12	1.978183	0.29461	0.0012028	0.0071085
beta.13	2.129820	0.29206	0.0011923	0.0072076
beta.14	−0.351238	0.42597	0.0017390	0.0071344
beta.15	−80.970151	58.79299	0.2400214	0.4011628
beta.1f	2.966160	0.28302	0.0011554	0.0070137
beta.23	0.277871	0.13035	0.0005321	0.0011083
beta.24	−1.598005	0.23596	0.0009633	0.0014912
beta.25	−5.229981	1.26970	0.0051835	0.0080808
beta.2f	1.278972	0.11052	0.0004512	0.0009751
beta.34	−1.422282	0.23587	0.0009629	0.0014378
beta.35	−3.285867	0.54935	0.0022427	0.0031250
beta.3f	1.518051	0.11513	0.0004700	0.0007073
beta.45	−3.134961	1.33008	0.0054300	0.0089360
beta.4f	2.293788	0.29657	0.0012107	0.0016414
beta.5f	4.047865	1.29729	0.0052962	0.0081469
beta.DBHf	−0.026615	0.07674	0.0003133	0.0007314
beta.DBHs	0.190139	0.08749	0.0003572	0.0008317
beta.TPHf	−0.187436	0.07059	0.0002882	0.0006126
beta.TPHs	0.004739	0.08236	0.0003362	0.0007240

References

Ali, Q., Bauch, C.T., Anand, M., 2015. Coupled human-environment dynamics of forest pest spread and control in a multi-patch, stochastic setting. In: Doucet, D. (Ed.), PLoS One 10 (10), e0139353. http://dx.doi.org/10.1371/journal.pone.0139353, URL http://dx.plos.org/10.1371/journal.pone.0139353.

Amazing Tree Services, 2017. Tree removal cost in NJ. Amazing Tree Services URL https://atreeservicenj.com/tree-removal-cost.asp.

Andresen, A.X., Kurtz, L.C., Hondula, D.M., Meerow, S., Gall, M., 2023. Understanding the social impacts of power outages in North America: a systematic review. Environ. Res. Lett. 18 (5), 053004. http://dx.doi.org/10.1088/1748-9326/acc7b9, URL https://iopscience.iop.org/article/10.1088/1748-9326/acc7b9.

Audley, J.P., Fettig, C.J., Steven Munson, A., Runyon, J.B., Mortenson, L.A., Steed, B.E., Gibson, K.E., Jørgensen, C.L., McKelvey, S.R., McMillin, J.D., Negrón, J.F., 2021. Dynamics of beetle-killed snags following mountain pine beetle outbreaks in lodgepole pine forests. Forest Ecol. Manag. 482, 118870. http://dx.doi.org/10.1016/j.foreco.2020.118870, URL https://linkinghub.elsevier.com/retrieve/pii/S037811272031639X.

Bíl, M., Andrášik, R., Nezval, V., Bílová, M., 2017. Identifying locations along railway networks with the highest tree fall hazard. Appl. Geogr. 87, 45–53. http://dx.doi.org/10.1016/j.apgeog.2017.07.012, URL https://linkinghub.elsevier.com/retrieve/pii/S0143622817301819.

Bureau of Climate Change and Clean Energy, 2021. NJ Community Solar PV Siting Tool User Guide. New Jersey Department of Environmental Protection, URL https://www.state.nj.us/dep/aqes/docs/sstguide.pdf.

Bureau of Transportation Statistics, U.S. Department of Commerce, U.S. Census Bureau, Geography Division, 2016. TIGER/line Roads County-based (National)-National Geospatial Data Asset (NGDA) TIGER/line Roads County-based. U.S. Department of Transportation, USA, URL https://tigerweb.geo.census.gov/arcgis/rest/services/TIGERweb/Transportation/MapServer.

Casey, J.A., Fukurai, M., Hernández, D., Balsari, S., Kiang, M.V., 2020. Power outages and community health: a narrative review. Current Environmental Health Reports 7 (4), 371–383. http://dx.doi.org/10.1007/s40572-020-00295-0, URL http://link.springer.com/10.1007/s40572-020-00295-0.

Coder, K.D., 2014. Trees & Storm Wind Loads. Warnell School of Forestry & Natural Resources, University of Georgia, URL https://bugwoodcloud.org/resource/files/15113.pdf.

Crocker, S.J., Barnett, C.J., Butler, B.J., Hatfield, M.A., Kurtz, C.M., Lister, T.W., Meneguzzo, D.M., Miles, P.D., Morin, R.S., Nelson, M.D., Piva, R.J., Reimann, R., Smith, J.E., Woodall, C.W., Zipse, W., 2017. New Jersey Forests 2013. Technical Report, NRS-RB-109, U.S. Department of Agriculture, Forest Service, Northern Research Station, Newtown Square, PA, http://dx.doi.org/10.2737/NRS-RB-109, URL https://www.nrs.fs.fed.us/pubs/53471.

Depaoli, S., Clifton, J.P., Cobb, P.R., 2016. Just another Gibbs sampler (JAGS): Flexible software for MCMC implementation. J. Educ. Behav. Stat. 41 (6), 628–649. http://dx.doi.org/10.3102/1076998616664876, URL http://journals.sagepub.com/doi/10.3102/1076998616664876.

Duan, J.J., Larson, K., Watt, T., Gould, J., Lelito, J.P., 2013. Effects of Host plant and Larval density on intraspecific competition in Larvae of the Emerald Ash Borer (Coleoptera: Buprestidae). Environ. Entomol. 42 (6), 1193–1200. http://dx.doi.org/10.1603/EN13209, URL https://academic.oup.com/ee/article-lookup/doi/10.1603/EN13209.

Forest Inventory and Analysis, 2022. Design and Analysis Toolkit for Inventory and Monitoring web application. St. Paul, MN: U.S. Department of Agriculture, Forest Service, Northern Research Station, URL https://www.fs.fed.us/emc/rig/DATIM/index.shtml..

Gould, J.S., Murphy, T., Slager, B., Bauer, L.S., Duan, J., Petrice, T., 2020. Emerald Ash Borer, Agrilus planipennis (Fairmaire), Biological Control Release and Recovery Guidelines 2020. United States Department of Agriculture, p. 75.

Harmon, M.E., Bell, D.M., 2020. Mortality in Forested Ecosystems: Suggested Conceptual Advances. Forests 11 (5), 572. http://dx.doi.org/10.3390/f11050572, URL https://www.mdpi.com/1999-4907/11/5/572.

Hledik, R., Lazar, J., Schwartz, L., 2017. Distribution System Pricing with Distributed Energy Resources. Technical Report, LBNL–1005180, 1375194, Lawrence Berkeley National Lab, http://dx.doi.org/10.2172/1375194, URL http://www.osti.gov/servlets/purl/1375194/.

Hughes, W., Zhang, W., Bagtzoglou, A.C., Wanik, D., Pensado, O., Yuan, H., Zhang, J., 2021. Damage modeling framework for resilience hardening strategy for overhead power distribution systems. Reliab. Eng. Syst. Saf. 207, 107367. http://dx.doi.org/10.1016/j.ress.2020.107367, URL https://linkinghub.elsevier.com/retrieve/pii/S0951832020308565.

Liddiard, R., Gowreesunker, B.L., Spataru, C., Tomei, J., Huebner, G., 2017. The vulnerability of refrigerated food to unstable power supplies. Energy Procedia 123, 196–203. http://dx.doi.org/10.1016/j.egypro.2017.07.238, URL https://linkinghub.elsevier.com/retrieve/pii/S1876610217328096.

Lyttek, E.W., 2023. The Fate of Fraxinus spp. in New Jersey: A Physioeconomic Evaluation of the Forest System and Infrastructure Implications (Ph.D. thesis). Montclair State University, Montclair, NJ.

Lyttek, E., Lal, P., Nieddu, G., Forgoston, E., Wieczerak, T., 2019. Modeling *Agrilus planipennis* F. (Coleoptera: Buprestidae) spread in New Jersey. In: Schowalter, T. (Ed.), J. Econ. Entomol. 112 (5), 2482–2488. http://dx.doi.org/10.1093/jee/toz122, URL https://academic.oup.com/jee/article/112/5/2482/5496795.

McCullough, D.G., Siegert, N.W., 2007. Estimating potential Emerald Ash Borer (Coleoptera: Buprestidae) populations using Ash inventory data. J. Econ. Entomol. 100 (5), 1577–1586. http://dx.doi.org/10.1603/0022-0493(2007)100[1577:EPEABC]2.0.CO;2, URL http://openurl.ingenta.com/content/xref?genre=article&issn=0022-0493&volume=100&issue=5&spage=1577.

McRoberts, R.E., Bechtold, W.A., Patterson, P.L., Scott, C.T., Reams, G.A., 2005. The enhanced forest inventory and analysis program of the USDA forest service: Historical perspective and announcement of statistical documentation. J. Agricult. Forestry 5.

Mercader, R.J., McCullough, D.G., Storer, A.J., Bedford, J.M., Heyd, R., Siegert, N.W., Katovich, S., Poland, T.M., 2016. Estimating local spread of recently established emerald ash borer, Agrilus planipennis , infestations and the potential to influence it with a systemic insecticide and girdled ash trees. Forest Ecol. Manag. 366, 87–97. http://dx.doi.org/10.1016/j.foreco.2016.02.005, URL http://linkinghub.elsevier.com/retrieve/pii/S0378112716300160.

Mercader, R.J., Siegert, N.W., Liebhold, A.M., McCullough, D.G., 2009. Dispersal of the emerald ash borer, *Agrilus planipennis*, in newly-colonized sites. Agric. for Entomol. 11 (4), 421–424. http://dx.doi.org/10.1111/j.1461-9563.2009.00451.x, URL http://doi.wiley.com/10.1111/j.1461-9563.2009.00451.x.

Mercader, R.J., Siegert, N.W., Liebhold, A.M., McCullough, D.G., 2011. Influence of foraging behavior and host spatial distribution on the localized spread of the emerald ash borer, Agrilus planipennis. Popul. Ecol. 53 (2), 271–285. http://dx.doi.org/10.1007/s10144-010-0233-6, URL http://link.springer.com/10.1007/s10144-010-0233-6.

Moosewood Tree Service, 2017. The average cost of tree removal. URL https://www.moosewoodtreeservice.com/single-post/2017/03/05/the-average-cost-of-tree-removal.

New Jersey Board of Public Utilities (NJBPU), New Jersey Department of Environmental Protection (NJDEP), New Jersey Department of Transportation (NJDOT), New Jersey Department of Community Affairs (NJDCA), New Jersey Department of Labor and Workforce Development (NJDOL), New Jersey Economic Development Authority (NJEDA), NJ TRANSIT, 2019. 2019 New Jersey Energy Master Plan Pathway to 2050. State of New Jersey, URL https://www.nj.gov/emp/docs/pdf/2020_NJBPU_EMP.pdf.

Oberle, B., Covey, K.R., Dunham, K.M., Hernandez, E.J., Walton, M.L., Young, D.F., Zanne, A.E., 2018b. Dissecting the effects of diameter on wood decay emphasizes the importance of cross-stem conductivity in Fraxinus americana. Ecosystems 21 (1), 85–97. http://dx.doi.org/10.1007/s10021-017-0136-x, URL http://link.springer.com/10.1007/s10021-017-0136-x.

Oberle, B., Ogle, K., Zanne, A.E., Woodall, C.W., 2018a. When a tree falls: Controls on wood decay predict standing dead tree fall and new risks in changing forests. In: Bond-Lamberty, B. (Ed.), PLoS One 13 (5), e0196712. http://dx.doi.org/10.1371/journal.pone.0196712, URL https://dx.plos.org/10.1371/journal.pone.0196712.

Plummer, M., 2003. JAGS: A program for analysis of Bayesian graphical models using Gibbs sampling. In: Proceedings of the 3rd International Workshop on Distributed Statistical Computing, vol. 1. DSC 2003, Proceedings of DSC 2003, Vienna, Austria, pp. 1–10, URL http://www.ci.tuwien.ac.at/Conferences/DSC-2003/.

Poland, T.M., Chen, Y., Koch, J., Pureswaran, D., 2015. Review of the emerald ash borer (Coleoptera: Buprestidae), life history, mating behaviours, host plant selection, and host resistance. The Canadian Entomologist 147 (03), 252–262. http://dx.doi.org/10.4039/tce.2015.4, URL http://www.journals.cambridge.org/abstract_S0008347X15000048.

Poulos, H.M., Camp, A.E., 2010. Decision support for mitigating the risk of tree induced transmission line failure in utility rights-of-way. Environ. Manag. 45 (2), 217–226. http://dx.doi.org/10.1007/s00267-009-9422-5, URL http://link.springer.com/10.1007/s00267-009-9422-5.

Public Service Electric & Gas Co. (PSE&G), 2007. 69 kV Statewide Initiative. PSE&G, URL https://www.psegtransmission.com/reliability-projects/69kv#:~:text=Since%202007%2C%20PSE%26G%20has%20installed,miles%20will%20have%20been%20upgraded.

Schlesinger, R.C., 1990. *Fraxinus Americana* L. White Ash. Silvics of North America 2, 333–338, http://willow.ncfes.umn.edu/silvics_manual/volume_2/fraxinus/americana.htm.

Siegert, N.W., McCullough, D.G., Liebhold, A.M., Telewski, F.W., 2014. Dendrochronological reconstruction of the epicentre and early spread of Emerald Ash Borer in North America. In: MacIsaac, H. (Ed.), Divers. Distributions 20 (7), 847–858. http://dx.doi.org/10.1111/ddi.12212, URL https://onlinelibrary.wiley.com/doi/10.1111/ddi.12212.

Siegert, N.W., McCullough, D.G., Williams, D.W., Fraser, I., Poland, T.M., Pierce, S.J., 2010. Dispersal of *Agrilus planipennis* (Coleoptera: Buprestidae) from discrete epicenters in two outlier sites. Environ. Entomol. 39 (2), 253–265. http://dx.doi.org/10.1603/EN09029, URL https://academic.oup.com/ee/article-lookup/doi/10.1603/EN09029.

Siegert, N.W., Mercader, R.J., McCullough, D.G., 2015. Spread and dispersal of emerald ash borer (Coleoptera: Buprestidae): estimating the spatial dynamics of a difficult-to-detect invasive forest pest. The Canadian Entomologist 147 (03), 338–348. http://dx.doi.org/10.4039/tce.2015.11, URL http://www.journals.cambridge.org/abstract_S0008347X15000115.

State of New Jersey Department of Agriculture, Emerald Ash Borer, N.D., URL https://www.nj.gov/agriculture/divisions/pi/prog/emeraldashborer.html.

U.S. Geological Survey, 2019. NLCD 2016 USFS Tree Canopy Cover (CONUS). U.S. Geological Survey, URL https://www.mrlc.gov/downloads/sciweb1/shared/mrlc/metadata/nlcd_2016_treecanopy_2019_08_31.img.xml.

Wang, H., Seaborn, T., Wang, Z., Caudill, C.C., Link, T.E., 2021. Modeling tree Canopy height using machine learning over mixed vegetation landscapes. Int. J. Appl. Earth Obs. Geoinf. 101, 102353. http://dx.doi.org/10.1016/j.jag.2021.102353, URL https://linkinghub.elsevier.com/retrieve/pii/S030324342100060X.

Warwick, W., Hardy, T., Hoffman, M., Homer, J., 2016. Electricity Distribution System Baseline Report. U.S. Department of Energy, p. 120.

Wilson, B.T., Lister, A.J., Riemann, R.I., 2012. A nearest-neighbor imputation approach to mapping tree species over large areas using forest inventory plots and moderate resolution raster data. Forest Ecol. Manag. 271, 182–198. http://dx.doi.org/10.1016/j.foreco.2012.02.002, URL http://linkinghub.elsevier.com/retrieve/pii/S0378112712000710.

Wolfe, J., Jin, X., Bahr, T., Holzer, N., 2017. Application of softmax regression and its validation for spectral-based land cover mapping. Int. Arch. Photogramm. Remote Sens. Spatial Inf. Sci. XLII-1/W1, 455–459. http://dx.doi.org/10.5194/isprs-archives-XLII-1-W1-455-2017, URL https://www.int-arch-photogramm-remote-sens-spatial-inf-sci.net/XLII-1-W1/455/2017/.

Woudenberg, S.W., Conkling, B.L., O'Connell, B.M., LaPoint, E.B., Turner, J.A., Waddell, K.L., 2010. The Forest Inventory and Analysis Database: Database description and users manual version 4.0 for Phase 2. Technical Report, RMRS-GTR-245, U.S. Department of Agriculture, Forest Service, Rocky Mountain Research Station, Ft. Collins, CO, http://dx.doi.org/10.2737/RMRS-GTR-245, URL https://www.fs.usda.gov/treesearch/pubs/37446.